Atomisation of a pulsed jet: morphology and thin sheet rupture

Y. Kulkarni[1], R. Villiers[1], S. Zaleski*[1], C. Pairetti[1], M. Crialesi-Esposito[2], S. Popinet [1]

[1]Sorbonne Université, Institut Jean le Rond d'Alembert, France
[2]KTH Royal Institute of Technology, Sweden
*Corresponding author: stephane.zaleski@sorbonne-universite.fr

Abstract

Jet atomisation is a multi-scale phenomenon and hence a challenging problem for numerical simulations, even in isothermal and incompressible flow ([1] , [2]). In the present study, simulation of a pulsating dense cylindrical liquid oil jet injected into a stagnant air phase is performed at Reynolds number Re=5800, Weber number We=5555 and density ratio $r = 28$ using the Volume of Fluid (VoF) method and octree adaptive mesh refinement using the Basilisk code. A grid refinement higher 900 cells per initial jet diameter is achieved. This is, to our knowledge, the most detailed simulation, including of this type of flow. Simulations provide direct evidence of many underlying mechanisms, and the effect of pulsation [3], the characteristic sheet perforation due to droplet impact, and sheet rupture due to stretching and thinning. The numerical curvature provides a diagnostic of the presence of weak spots. After holes form from the weak spots, characteristic ligament networks develop. The probability distribution function (PDF) of the droplet sizes is obtained. It converges slowly with the minimum grid size (Δ) and has a bimodal character. The position of the two peaks shift towards smaller scales as Δ decrease, indicating the grid dependency of the mechanisms involved, with sheet perforation the likely culprit. At large scales, however the PDF is seen to be converging.

Keywords

Jet atomisation , weak spots, Volume of Fluid (VoF) method, octree adaptive mesh refinement.

Introduction

Atomisation refers to the breaking of a fluid mass into various small droplets and pieces, often of the microscopic size. Jet atomisation has wide applications like combustion, spray formation, disease spread, ocean waves etc. One of the main scientific interest in the atomisation studies is to understand the various mechanisms leading to the droplet formation and predict the droplet size distribution. This is going to be the main focus of the present work. Some previous articles, as the work of Shinjo and Umemura [4], describe different atomization regimes at moderate Reynolds and Weber numbers using a second-order level-set method and described in detail the jet tip deformation and fragmentation process and how they interact with the vortex dynamics. More fundamental studies by Jarrabashi *et. al.* ([5], [6]) analyzed the deformation of periodic cylindrical jets for a broader spectrum of flow regimes. They analyze the effect of vortex dynamics on the development of instabilities along with the jet core. Using similar methods, Zandian *et. al.* [7] described the breakup process on planar jets and how the fragmentation modes develop for a different set of parameters. Even if these analyses characterize the growth of interface instabilities in detail, they do not give further insights on how this process impacts on the final drop size distribution. Besides these difficulties, DNS is still used to study early atomization stages on fuel injection problems. Ling *et al.* [8] , Zhang Y. *et al.* [9] and Zhang B. *et al.* [10] applied the VOF technique with Adaptive Mesh Refinement (AMR) to analyze the primary atomization of diesel, biodiesel, and gasoline on injection problems at moderate speeds. Through a complete statistical characterization of the cases, these works describe the overall evolution of the fuel spray. These simulations employed the *Basilisk* C platform, by Popinet and collaborators [11]; we obtained the results presented in this manuscript using an updated version of these numerical tools.

Thanks to the TGCC supercomputers and *Basilisk* visualisation tools, we are able to reach resolution up to 900 cells per initial diameter and are able to have some insights on the droplet formation mechanisms. We also see the droplet size distribution to be grid dependent and use the numerical curvature ripples on the interface to find out the likely culprit for the numerical droplets as seen in the results section.

Methodology

The mathematical model is based in the mass and momentum conservation equations for incompressible and isothermal flow:

$$\nabla \cdot \vec{u} = 0 \tag{1}$$

$$\frac{\partial \rho \vec{u}}{\partial t} + \nabla \cdot (\rho \vec{u}\vec{u}) = -\nabla p + \nabla \cdot (2\mu \mathbf{D}) + f_\sigma \tag{2}$$

where $\vec{u}(\vec{x},t)$ is the velocity field and $p(\vec{x},t)$ is the pressure field. The tensor $\mathbf{D}$ is defined as $\frac{1}{2}\left[\nabla\vec{u} + (\nabla\vec{u})^T\right]$. The density and viscosity of the flow are noted as ρ and μ respectively. The last term on the right-hand side on the Navier-Stokes Equation 2 represents the surface tension force:

$$f_\sigma = \sigma\kappa\vec{n}_s\delta_s \tag{3}$$

which depends on the surface tension coefficient σ and the interface shape, particularly on its curvature κ and normal $\vec{n}_s$. The Dirac function δ_s indicates that the force only acts at the free surface.

We consider the phase distribution of the flow using a color function $c(\vec{x},t)$ that takes value $c(\vec{x}_p,t) = 1$ if the point p is filled with one phase and $c = 0$ otherwise. The transport equation for this function is:

$$\frac{\partial c}{\partial t} + \nabla \cdot (c\vec{u}) = c\,\nabla \cdot (\vec{u}). \tag{4}$$

In the context of incompressible flow, the right-hand side is equal to zero due to Equation (1). We should mind that the c function implicitly defines the interface at its discontinuity surface, defininng also the δ_s, $\vec{n}_s$, and κ fields.

The numerical schemes used here is exactly same as in [10]. One can refer to [12] to look how the method is well balanced.

Simulations setup

We analyze the atomization of a circular jet injected on a gas-filled cubical chamber considering incompressible isothermal flow. The dimensionless groups relevant on this problem are:

$$We = \frac{\rho_l U^2 D}{\sigma} \qquad Re = \frac{\rho_l U D}{\mu_l} \qquad \rho^* = \frac{\rho_l}{\rho_g} \qquad \mu^* = \frac{\mu_l}{\mu_g} \tag{5}$$

where ρ_l and ρ_g are the densities of each phase, in this case, liquid and gas respectively. The viscosity coefficients are noted by μ_l and μ_g. σ is the surface tension coefficient, U is the injection mean velocity and D is the nozzle diameter. The Reynolds and Weber numbers can be computed for both phases. The characteristic time based on the problem kinematics is $t_c = (D/U)$.

The boundary condition on the injection plane ($x = 0$) imposes the no-slip condition everywhere except on the liquid section ($\sqrt{y^2 + z^2} < D_{inj}/2$) where the injection velocity is:

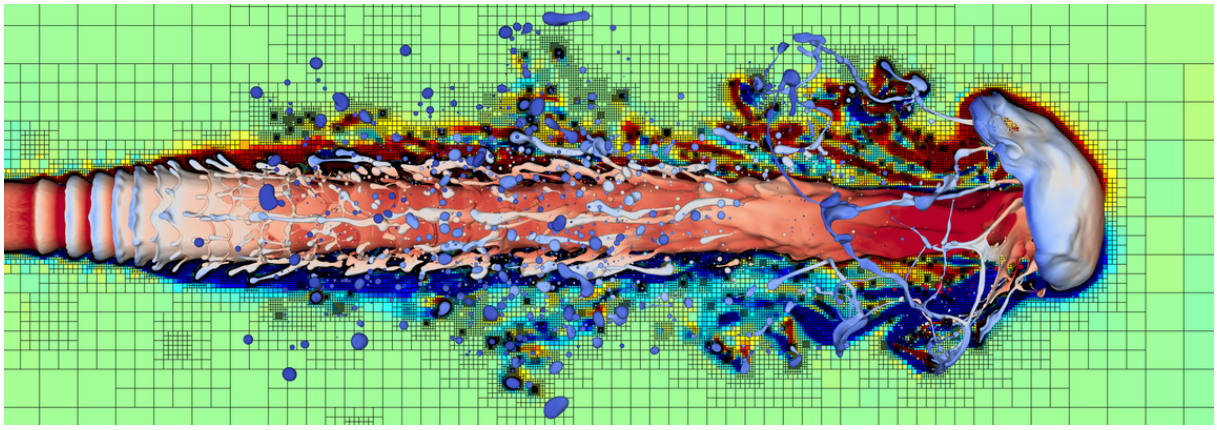

Figure 1. Developed atomisation jet. The interface is colored by axial velocity and the background represents vorticity.

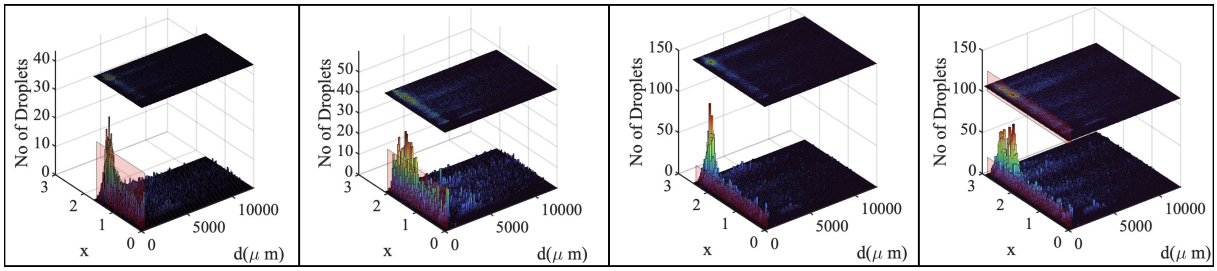

Figure 2. Surface histograms showing droplet size distribution at the intervals t = 2.0 , 2.5 , 3.0 and 3.5 (left to right).

$$u_x(t) = U\ [1 + A\sin(\omega_p t)] \tag{6}$$

On the remaining cube sides, we allow free outflow: $\partial_n \vec{u}_\Gamma = 0$ and $p_\Gamma = 0$.

Results and Discussion

We start by a general description of the morphology as seen from the fully developed jet in figure 1. The pulsation accelerates the formation of hydrodynamic instabilities in the region near the injection section. As the jet advance, a typical mushroom like structure is developed. Note that this mushroom is the main source of the droplets. This is seen from 3d histograms in figure 2 where the peak is always around the position of the mushroom cap. Once the jet has crossed a certain length, the effect of the pulsation is lost and long ligaments are seen. As seen from the coloring in figure 1, these ligaments have a velocity gradient and continue to stretch before generating several droplets.

Figure 3a shows the probability density function (pdf) of droplet diameter. We see the pdf is bimodal and depends highly on the grid size. Close examination suggests that the pdf converge in the tail region for large droplets (inset). Figure 3b suggests that although both the peaks of bimodal distribution is shifting with the grid refinement, the peak corresponding to the larger one shifts slowly, indicating some convergence for larger droplets.

To diagnose the mechanism responsible for the formation of small numerical droplets, we color the interface by curvature. By examining closely the weak spot rupture (thin sheet rupture), we see that just before the rupture happens, there are curvature oscillations indicating the ripples scaling with grid size. These ripples result in a number of small numerical droplets. This whole process is shown in figure 4.

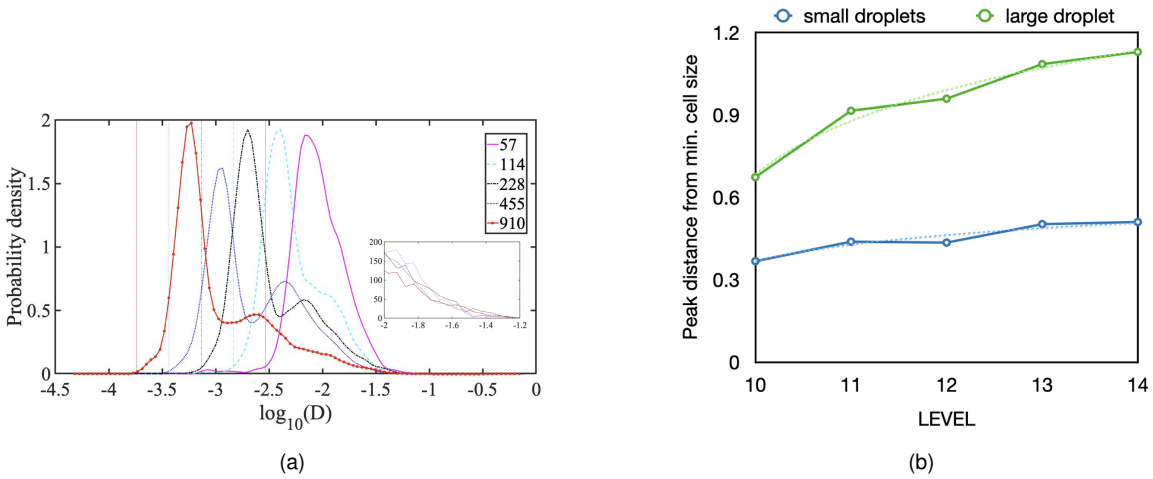

Figure 3. (a) Probability density function for droplet size distribution at various resolution (legend). The vertical lines represent the minimum cell size. (b) The distance of the two peaks from the minimum cell size

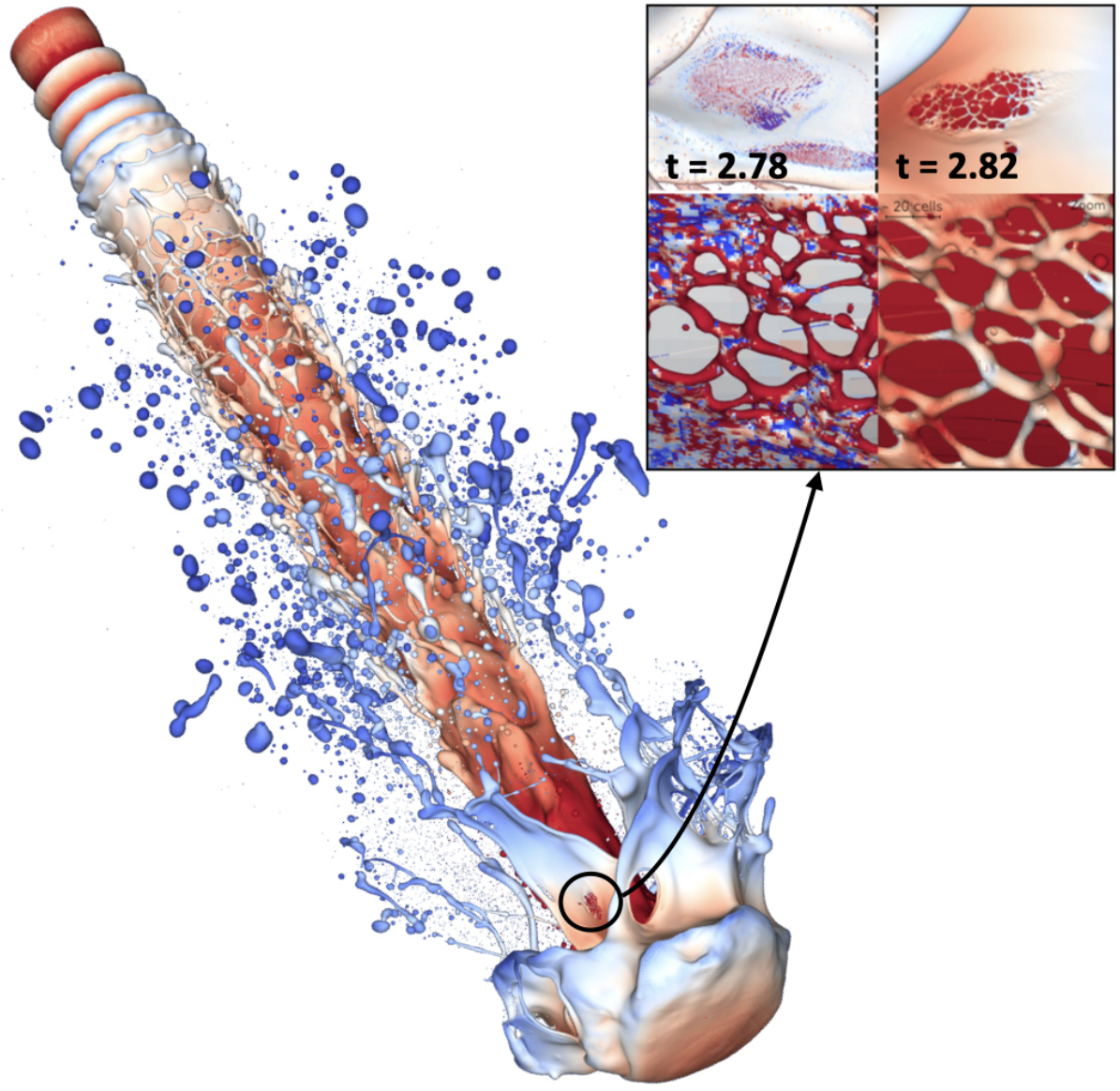

Figure 4. A zoomed in view of weak spot to show the numerical rupture captured in our simulations. The interface is colored by the axial velocity and curvature (inset).

Acknowledgements
We acknowledge support from ERC Adv grant TRUFLOW, and PRACE and GENCI grants of CPU. Simulations performed on Irene-Rome at TGCC, France.

References

[1] R. D. Reitz, F. V. Bracco, Mechanism of atomization of a liquid jet, Physics of Fluids (1982).
[2] M. Gorokhovski, M. Herrmann, Modeling Primary Atomization, Annual Review of Fluid Mechanics (2008).
[3] X. Yang, A. Turan, Simulation of liquid jet atomization coupled with forced perturbation, Physics of Fluids (2017).
[4] J. Shinjo, A. Umemura, Simulation of liquid jet primary breakup: Dynamics of ligament and droplet formation, International Journal of Multiphase Flow (2010).
[5] D. Jarrahbashi and W. A. Sirignano, Vorticity dynamics for transient high-pressure liquid injection, Physics of Fluids (2014).
[6] D. Jarrahbashi, W. Sirignano, P. Popov and F. Hussain, Early spray development at high gas density: Hole, ligament and bridge formations. Journal of Fluid Mechanics (2016).
[7] A. Zandian, W. Sirignano and F. Hussain Understanding liquid-jet atomization cascades via vortex dynamics. Journal of Fluid Mechanics (2018).
[8] Y. Ling, D. Fuster, S. Zaleski, G. Tryggvason, Spray formation in a quasiplanar gas-liquid mixing layer at moderate density ratios: A numerical closeup, Physical Review Fluids (2017).
[9] Y. Zhang; B. Sun; H. Fang; D. Zhu; L. Yang; Z. Li Experimental and Simulation Investigation on the Kinetic Energy Dissipation Rate of a Fixed Spray-Plate Sprinkler, Water (2018).
[10] B. Zhang, S. Popinet, Y. Ling, Modeling and detailed numerical simulation of the primary breakup of a gasoline surrogate jet under non-evaporative operating conditions, International Journal of Multiphase Flow (2020).
[11] S. Popinet, Basilisk code, (2014). URL: http://basilisk.fr/
[12] S. Popinet, Numerical Models of Surface Tension, Annual Review of Fluid Mechanics (2018).